Available online at www.eccomasproceedia.org
Eccomas Proceedia COMPDYN (2021) 847-859

ECCOMAS
Proceedia

COMPDYN 2021
8th ECCOMAS Thematic Conference on
Computational Methods in Structural Dynamics and Earthquake Engineering
M. Papadrakakis, M. Fragiadakis (eds.)
Streamed from Athens, Greece, 28 - 30 June 2021

STRUCTURAL CONCEPTS IN THE DESIGN OF MASONRY-INFILLED STEEL FRAMES

D. Šokić[1], D. Markulak[1], T. Dokšanović[1], I. Radić[1]

[1] Josip Juraj Strossmayer University of Osijek, Faculty of Civil Engineering and Architecture,
Vladimira Preloga 3, HR – 31000 Osijek, Croatia.
e-mail: (dsokic, markulak, tdoksanovic, radic)@gfos.hr

Abstract

Despite numerous research studies conducted in the field of masonry-infilled steel (and concrete) frames, there is still no adequate codified design method. There is, however, a consensus that masonry-infilled frames should be treated as potentially hazardous earthquake context structural solutions. While masonry infill has positive effects on steel frames, which are often neglected in design, adverse effects cannot be overlooked. Over the last decade, several structural solutions aimed to improve the overall structural behavior of these interactive composite systems were proposed and tested in laboratory conditions. It is not rare that these approaches are opposite to each other, which additionally stresses the fact that there is a need for recognition and validation of the key structural directions. Among various proposed design options, the authors are very interested in those which tend to include the beneficial effect of masonry infill, but at the same time preserve desired ductile behavior of steel frames, all by using simpler and easy to apply structural solutions. Some of them are already proposed by the authors, which are discussed in the paper, along with a summary and comparison of contemporary structural solutions in steel masonry-infilled frames, as an important step towards codification.

Keywords: steel-masonry, composite structure, earthquake design, structural solutions

1 INTRODUCTION

Masonry blocks, due to easy production, installation and accessibility are the most widespread infill type in frame structures, especially in Europe. It is known that the presence of masonry infill can significantly increase stiffness and strength, but it can also limit the ductile behavior of frames in case of higher lateral load such as an earthquake. Consequently, researchers evaluate the contribution of the masonry infill and their influence on the frame, and through this process started to develop innovative structural concepts to mitigate the negative effects of

ISSN:2623-3347
Peer-review under responsibility of the organizing committee of COMPDYN 2021.
doi:10.7712/120121.8529.19075

masonry infill. Based on this, numerous structural concepts in the design of infilled frames can be found, aimed to improve the overall interaction between infill and frame. The typical solutions are application of various infill types (i.e. using soft or strong materials for infill), modification of the failure mechanisms, reinforcing of the infill etc. These methods can be generally categorized into two groups [1]:

- Strengthening of the masonry infill through which the composite structure frame+infill behaves as a monolithic construction.
- Limiting frame-infill interaction through which both monolithic and separate behavior of the frame and the infill may be observed.

The strengthening methods are mainly characteristic for concrete frames, while the limited interaction is characteristic for steel frames, although some deviations can be found in the literature review that follows.

One of the most natural types of strengthening infill was covered in the study done by Pul and Arslan [2]. They used and compared plastered, non-plastered, and wire-plastered masonry walls made from hollow clay brick. Results show that plaster and wire plaster enhance load-carrying capacity and ductility, which is good since most of the masonry application includes a plaster surface layer. Jebadurai et al. [3] focused their research on enhancing the bond strength between masonry units in RC frames by adding a different percentage of styrene-butadiene rubber latex in the mortar. Experiments showed that using modified mortar with a certain percentage of latex increased ductility by 12.90%. Binici et al. [4] investigated a well-known infill type, autoclaved aerated concrete, but with an improvement regarding infill execution - metal slider connectors in AAC blocks. Due to this slider connector, the interaction between the RC frame and infill is limited. As a result, the in-plane damage is postponed at higher drift ratios and the out-of-plane damage is limited. Ruey-Shyang Ju et al. [5] studied separation of RC infill walls from steel moment frames by making vertical slits and leaving a horizontal gap between the upper steel beam and the infill RC wall. Results of this study showed that proper design and arrangement of slits can absorb the relative deformation between the column and infill wall and it can isolate the separated wall from damage. Innovative isolation of masonry infill from steel frames is presented by Tsantilis and Triantfillou [6], as they use a cellular material (foamed polyethylene) placed in the frame-infill interface. The cellular material has high deformation capabilities which mitigate interaction between the steel frame and masonry infill in the initial phase of loading. As loads get higher the cellular material gets fully compressed and the diagonal compression strut is activated. M. Mohammadi et al. [7] investigated three different techniques to improve steel frame ductility: (i) cornerless infill, (ii) column fuse, and (iii) infill fuse (applied metal sheets in infill layer to provide horizontal sliding). The infill fuse method has shown a significant increase of ductility with no significant cracks or corner crushing up to 7.1% drift. Preti and Bolis [8], and Morandi et. al. [9], tested the steel frame by dividing infill into more subpanels with wooden boards placed in the horizontal and vertical direction. Each of those configurations has shown a serious reduction of infill stiffness and strength in comparison to the reference masonry infill. Marinkovic and Butenweg [10] developed a system named INODIS, in which an elastomeric cellular material is used around the infill frame surface. Besides reduced interaction between the frame and infill, it reduced stress and infill damage. Moreover, the INODIS system allowed higher interstory drifts (more than 3%). Silva et. al [11] developed new units with an interlocking tongue and groove configuration, with vertical reinforcement. Due to reinforcement, an increase of lateral resistance up to 40% in relation to the bare frame was observed. Aliaari and Memari [12] introduced an idea of seismic isolator subframes attached to the structural frame, which they named SIWIS - a system made of one horizontal and two vertical sandwiched light-gauge steel members with a brittle element inside. They aimed to reduce the story drift at low and moderate lateral loads through the beneficial

effect of infill (higher stiffness and strength), while at higher lateral loads the brittle element acts as a „fuse“ in which they attempt to separate infill-frame interaction. Misir et al. [13] researched a new potential infill type without layers of mortar between them - locked brick. Besides the cracks in plaster, locked bricks stay intact and are less damaged in comparison to standard infill. Markulak et. al [14] presented a newly developed masonry unit for infill with lower initial stiffness and strength with a tendency to achieve minimal detrimental influences on the frame, while at the same time acknowledging environmental aspects.

Through a brief overview of structural concepts, it can be observed that there are numerous efforts of researchers to provide adequate solutions to undesired structural behavior of masonry infilled frames. Although some of them are challenging in terms of the execution (e.g. complexity, extra work hours, overall economic costs), provided experimental results and conclusions are of significant importance. The authors of this paper also conducted various experiments on infilled-steel frames in the mentioned direction, some of them accompanied with corresponding numerical models. The main intention being to keep favorable properties of the masonry while maintaining the steel frame ductile behavior at higher lateral loads. For calibration of experimental results various numerical models are used, with more details given in [15, 16]: (i) single equivalent strut (SSM), (ii) three equivalent struts (MSM), (iii) infill panel element (SPM), (iv) micro-model (AMM).

This paper presents findings regarding the influence of the different types of infill on steel frames. This is done through a short literature overview, to correlate the purpose of different experiments. Conducted experiments will be presented along with calibrated numerical results and grouped based on infill type - hollow clay brick (strong infill), autoclave aerated block (weak infill), the combination of those two (innovative solution proposed by authors), and newly developed RBA-EP unit (new structural concept proposed by authors).

2 STEEL FRAMES INFILLED WITH CLAY HOLLOW AND SOLID UNITS

Masonry units are the most used infill in conducted experiments [6, 17, 18, 19, 20, 21]. The masonry infill can be grouped depending on the unit configuration, i.e. as hollow clay block (HC) and solid clay block (SC). Despite different configurations, both types of blocks considerably increase initial stiffness and lateral bearing capacity. In most of the infilled frames, a diagonal compression strut mechanism is developed, accompanied with horizontal sliding along the bed joints. Horizontal shear sliding is the predominant mode of cracking in most of the experiments where the mortar is of insufficient strength. Most of the cracks are developed through the bed and head joints. Diagonal cracking or corner crushing is observed as an ultimate failure mechanism. Besides corner crushing, spalling of blocks is also observed.

The experimental setup that the authors executed consisted of three specimens of a one-bay, one-story rigid steel frame infilled with hollow clay units, designated as RF-C-i, with frame dimensions of 2176x1613 mm [1, 15]. Hollow clay units’ average vertical and horizontal compressive strengths were 13.10 MPa and 2.10 MPa, respectively. Cement-lime mortar was utilized, with an average compressive strength of 5.02 MPa. The average value of compressive strength and modulus of elasticity of masonry wallets made from hollow clay units was 2.0 MPa and 4613 MPa, respectively. The steel frame is constructed using HE 120 A profiles for columns and beam with steel grade S275. All the properties of the steel frame were identical for all three specimens. The loading protocol of each specimen consists of two types of loading. At the initial stage up to yielding, quasi-static and cyclic loads were applied stepwise in a series of increments of 10 kN. After yielding, the load was applied as a displacement control in which displacements were increased by increments of 1 mm until a drift of 1.0-2.0% was reached.

Table 1 presents the key parameters that were tested - initial stiffness (S_0), the load at the start of yielding (F_y), ultimate load (F_u), and corresponding maximum displacement (d_{max}) in

which (F_y) represents the onset of the first significant crack. The mean initial stiffness was determined as 31.3 kN/mm and the first significant crack was observed at loads of 59 kN, 70 kN, and 51 kN. For all three specimens, the first crack occurred in the middle of the infill with cracks through the mortar. The average maximum achieved load was 135 kN, while the average maximum displacement at a corresponding drift ratio of 1.39% was 22.46 mm. It should be noted that the steel frame on tested specimens did not exhibit significant plastic deformations. By exceeding the compression strength of infill diagonal cracking occurred with the appearance of shattering and spalling of hollow clay units. Alongside aforesaid failure, bed joint sliding shear failure was also observed. Those types of failure mechanisms are also noticed for the same infill type but with less pronounced corner crushing in [6]. An identical failure mechanism is observed with solid clay units in [19], but with permanent plastic deformation at the bottom of columns.

Experimental results					Numerical results		
Labels	S_0 (kN/mm)	F_y (kN)	F_u (kN)	d_{max} (mm)	Model	S_0 (kN/mm)	F_u (kN)
RF-C-1	32.07	59	139	21.33	SSM	31	134
RF-C-2	27.89	70	139	21.87	MSM	29	124
RF-C-3	34.00	51	128	24.20	SPM	37	140
RF-C_{av}	31.30	60	135	22.46	AMM	31	130

Table 1: Experimental and numerical results of specimens with strong infill

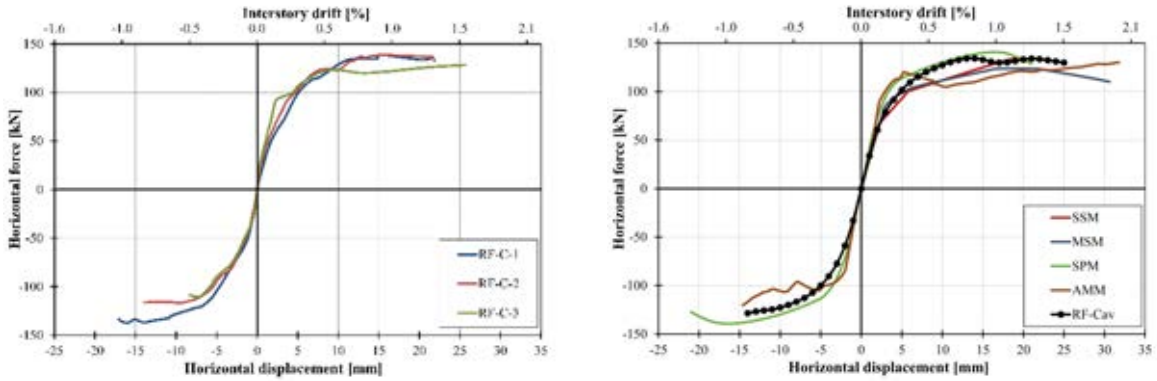

a) Experimental hysteresis envelope curves b) Analytical hysteresis envelopes curves

Figure 1: Comparison of experimental hysteresis envelopes (a) and analytical results for C-i series (b)

Regarding numerical models, Table 1 shows a good agreement with experimental results in terms of initial stiffness. SSM and AMM models provide the best agreement, while the SPM method overestimates the initial stiffness (19%). Considering the ultimate lateral load, SSM again provides the best agreement with only a 1% difference. MSM and AMM models underestimated the ultimate lateral load by 8% and 4%, respectively. Figure 1 presents hysteresis envelope curves for each calibrated numerical model, along with experimental results. SSM and MSM models predict a bilinear behavior, although the MSM model provides a smoother envelope. The envelope curve obtained from the AAM model matches very well with experimental initial stiffness, although lateral loads are somewhat lower. The envelope curve obtained from SPM shows a good fit for experimental results overall. It can be concluded that all calibrated models provide a good fit regarding infill made of HC units.

3 STEEL FRAMES INFILLED WITH AUTOCLAVED AERATED UNITS

Autoclaved aerated concrete block (AAC) is a light-weight unit with a significantly lower compressive strength compared to HC and SC units. Due to their small weight, they are favorable units to use as an infill, especially in terms of seismic design. Experiments based on AAC units as infill in steel frames are presented in [22-24], where it is confirmed that they increase initial stiffness and ultimate load capacity. They have lower compressive strength and infill tends to crack at very low loads, as shown in [24] where cracks developed diagonally passing through AAC units and mortar. All of the mentioned three studies report yielding of the steel frame and in [22, 23] local buckling of the flange in the base of the column was reported. Furthermore, in [23] AAC panels crushed and began to spall at similar displacement when the top flange of the column buckled. Contrary to that, in [24] AAC blocks did not fail even at the drift of 1.4% when the test was stopped due to the yielding of the steel frame, but without out-of-plane instability.

The experimental setup that the authors executed consisted of three specimens with the same experimental arrangement as described for RF-C-i specimens (Section 2), with samples designated as RF-A-i [1, 15]. Detailed results of testing individual AAC units and wallets are available in [15] - units vertical compression strength was 2.11 MPa, mortar glue compression strength 9.13 MPa, wallets vertical compressive strength and modulus of elasticity 1.21 MPa and 1174 MPa, respectively.

The experimental results are given in Table 2, from which it can be observed that RF-A-i specimens have lower initial stiffness than RF-C-i specimens (60%). The mean initial stiffness was 19.83 kN/mm. Sample RF-A-1 stands out in regards to initial stiffness (Fig 2.), which can be attributed to inaccuracies during erection [15]. Despite an earlier onset of cracking (average of 51 kN) in relation to RF-C-i specimens, the infill remained compact. The maximum achieved load is 146 kN, with a maximum displacement of 28.01 mm at a corresponding drift ratio of 1.74%. It can be noticed that maximum loads are higher than for RF-C specimens, despite lower mechanical characteristics of AAC blocks. This could be due to the higher compressive strength of bonded glue. Attained ultimate drift ratio of 1.74% signifies that there is plastic deformation at the steel column base.

Experimental results					Numerical results		
Labels	S_0 (kN/mm)	F_y (kN)	F_u (kN)	d_{max} (mm)	Model	S_0 (kN/mm)	F_u (kN)
RF-A-1	26.23	54	152	26.83	SSM	13	152
RF-A-2	15.07	51	139	30.73	MSM	15	123
RF-A-3	17.50	49	146	26.47	SPM	19	134
RF-A_{av}	19.83	51	146	28.01	AMM	23	141

Table 2: Experimental and numerical results of the specimen with weak infill

The failure mode of the RF-A-i specimens is similar to RF-C-i specimens, but with less intensity of diagonal cracking, i.e. infill was compact with more minor cracks and without extensive crushing and separation from the steel frame with horizontal sliding along the bed joints.

Initial stiffness obtained by the SSM model does not coincide with experimental results and the SPM method provides the best agreement in this regards (deviation of 10%). The AAM model slightly overestimates the value of the initial stiffness. In terms of ultimate lateral load MSM, SPM and AMM models underestimate values regarding all three specimens, while the SSM model overestimates the ultimate lateral load concerning all specimens. For a detailed

comparison of behavior between experimental and numerical results Figure 2 presents hysteresis envelope curves for each numerical model.

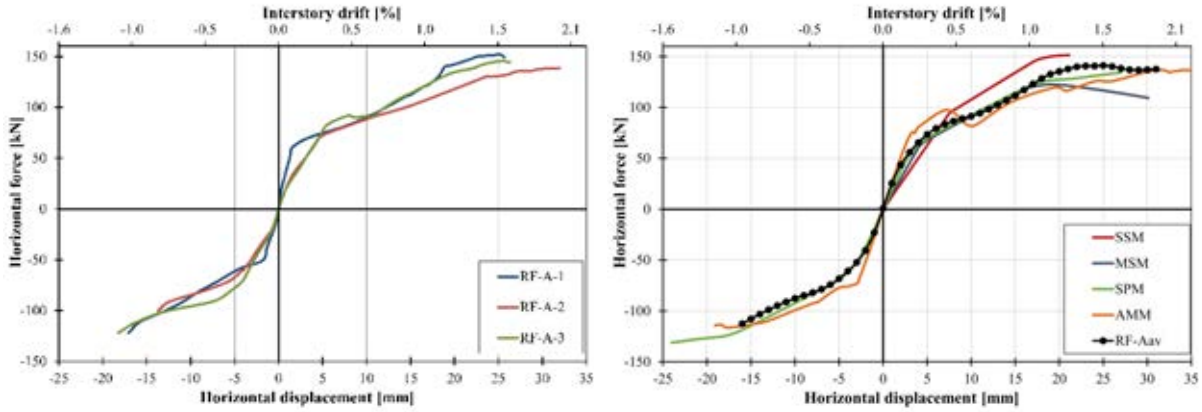

a) Experimental hysteresis envelopes curves b) Analytical hysteresis envelope curves

Figure 2: Comparison of experimental hysteresis envelopes (a) and analytical results for A-i series (b)

4 STEEL FRAMES WITH COMBINATION OF CLAY AND AAC UNITS INFILL

This innovative structural concept, presented in [15], is based on limiting (reducing) the interaction between the masonry infill and the steel frame. It is based on the solution of using a combination of AAC and HC units in an infill, to utilize the lower and higher compressive strengths in areas where needed. Weak infill is placed near the column-masonry interaction area are to act as a fuse. Since the AAC units have significantly lower compressive strength, the assumption was that those units will fail first and the steel frames will be preserved from further negative impacts of infill. This solution is distinct by two types of behavior: the monolithic at the initial stage of loading (higher initial stiffness and bearing capacity) and after the separation happens a steel frame dominated behavior. A similar solution can be found in [5, 6, 10, 12] where there are also two stages of behavior, but the initial stage is designed to be dominated by the steel frame, and at higher loads, the steel frame starts to interact with the masonry infill.

The executed experimental programme consisted of three specimens of steel frames infilled with combined HC and AAC units. The AAC units were additionally weakened with drilled holes of different diameters (ø54, ø74, ø84) to alter their compressive strength - vertical compressive strength of 2.11 MPa (for AAC=ø54), 2.03 MPa (for AAC= ø74) and 1.6 MPa (for AAC=ø84) are determined. The experimental setup and loading protocol were the same as for RF-C-i and RF-A-i testing (Section 2 and 3). The influence of holes is significant and it should be emphasized that three specimens of this type of infill represent three different systems.

Experimental results presented in Table 3 show that specimens RF-CA-i, in general, provide higher initial stiffness than RF-A samples, which can be attributed to the higher influence of clay blocks. Despite the higher initial stiffness, cracks were observed much earlier in all three specimens and mostly in AAC blocks. RF-CA-1 achieved the desirable behavior (higher initial stiffness and bearing capacity in the initial loading stage regarding bare frame) whereas the weakening of AAC blocks for other samples was excessive with premature separation occurring. The main difference between RF-A and RF-CA-1 was that the steel frame did not exhibit plastic deformations and the central part of masonry infill was practically undamaged in RF-CA-1. Despite the undamaged infill, proper attention should be paid to the out-of-plane restraint, which can be prevented from falling out-of-plane by construction provisions [1,15]. The maximum obtained load of RF-CA-1 was 106 kN, while the maximum measured displacement was

15.27, which corresponds to a drift ratio of 0.95%. Table 3 presents the numerical results. Concerning the initial stiffness, SSM provides the poorest fit to experimental results (deviation of 38%) and the closest fit is provided with the SPM model. Figure 3 illustrates experimental and numerically predicted behavior, from which the desired effect of pronounced bilinear behavior can be seen. The AAM calibrated envelope curve almost perfectly matches with results for RF-CA-1, which is also true regarding cracks forming in the infill [1, 15].

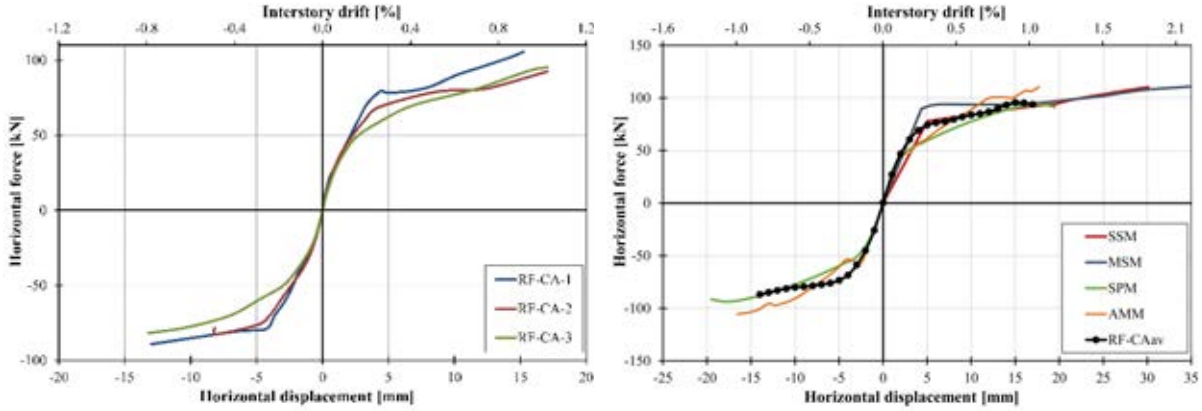

a) Experimental hysteresis envelope curves b) The analytical hysteresis envelope curve

Figure 3: Comparison of experimental hysteresis envelopes (a) and analytical results for CA-i series (b)

Experimental results					Numerical results		
Labels	S_0 (kN/mm)	F_y (kN)	F_u (kN)	d_{max} (mm)	Model	S_0 (kN/mm)	F_u (kN)
RF-CA-1	23.93	39	106	15.27	SSM	15	94
RF-CA-2	23.26	40	93	17.15	MSM	21	94
RF-CA-3	19.49	50	95	17.16	SPM	22	92
					AMM	25	106

Table 3: Experimental and numerical results of the specimen with strong-weak infill

5 STEEL FRAMES WITH NEWLY DEVELOPED UNITS INFILL

Previous experiments indicate that achieving higher compressive strength and modulus of elasticity of the masonry units is not of great importance to improve the behavior between infill and steel frame, especially in terms of achieving higher ultimate load. Hence, the lower stiffness and strength of the masonry unit can also benefit a steel-masonry infill system. Having this in mind, a new structural solution to this composite structure is proposed by developing a masonry unit that will mitigate negative effects on the steel frame, while preserving positive aspects of an infilled system. Consequently, masonry units from self-compacting concrete (SCC) were developed at the Faculty of Civil Engineering and Architecture in Osijek.

The newly developed masonry block is presented in previous research [25], with the main idea being to manipulate the composition of the developed block. For that purpose, self-compact concrete (SCC) was selected and to reduce stiffness and strength, replacement of natural aggregate was done with recycled crushed brick (RB) and ground expanded polystyrene (GEP) – RBA-EP. The mean value of compressive strength of RBA-EP is 4.04 MPa, which is in comparison with the hollow clay bricks 70% lower and 48% higher compared with AAC block. The modulus of elasticity obtained from wallets made of RBA-EP is 2746 MPa, which is in comparison to wallets made of hollow clay brick and AAC 60% lower and 57% higher, respectively. When considering the weight, the masonry panel made of RBA-EP, AAC, and hollow clay

brick was 293.2 kg, 140.0 kg, and 264.0 kg respectively. For the testing in frames, two types of RBA-EP units are made (Figure 4) - RBA-EP-Type A as a standard unit and RBA-EP-Type B as a weakened unit without one vertical wall along the sidewall.

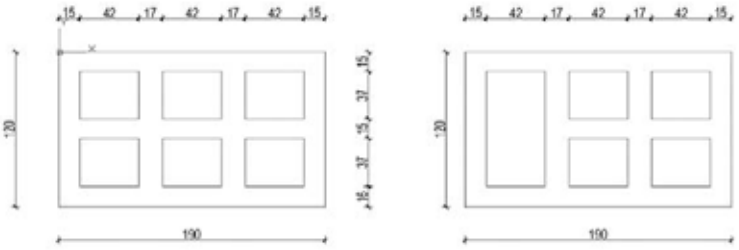

Figure 4: Configuration of Type A (left) and Type B (right)

Experimental testing of steel frames infilled with newly developed masonry units was done in two series, in a one-bay, one-story rigid steel frame and a pinned steel designated as RF and PF, respectively (dimensions 2332x1683 mm as in previous cases). The rigid steel frame was constructed of HE 120 A profile for columns and beam, while the pinned frame was constructed of HE 280 A profiles. Besides one bare rigid frame (RF) as a control specimen, the rest of the specimens were done as two samples per series. RF-M was infilled with RBA-EP-Type A units only whereas RF-MF was infilled with both RBA-EP-Type A and Type B units. RBA-EP-Type B units were placed at the column-masonry contact, which attempted to be used as a fuse. PF-MF was infilled with RBA-EP-Type A units in the pinned steel frame. All specimens were bonded with M5 class mortar. The loading protocol consists of a horizontal load applied by displacement control with increasing displacement by 0,5mm in each consecutive stage.

Experimental results reported in Table 4 present key parameters that were tested - initial stiffness (S_0), load at start of yielding (F_y), ultimate load (F_u), and corresponding maximum pushover displacement (d_{max}). RF-M and RF-MF have the highest initial stiffness of the tested specimens. Average values of initial stiffness for RF, RF-M, RF-MF, and PF are, respectively, 3.1 kN, 14.4 kN, 14.3 kN, and 7.6 kN. According to the highest initial stiffness, the highest ultimate loads are obtained for RF-M and RF-MF specimens, while the lowest is for PF specimen. The similarity of RF configuration is observed in the value of the horizontal load at start of yielding (the average F_y for RF, RF-M, and RF-MF was respectively, 69.4 kN, 64.9 kN, and 68.4 kN [14]). Although those values are close, the achieved horizontal displacements at the corresponding F_y were significantly different. Average horizontal displacement d_y for RF, RF-M, and RF-MF were, respectively, 23.8 mm, 7.4 mm, and 6.2 mm. Horizontal load F_y of PF-M configuration deviates from the other specimens and it is significantly lower (average F_y 21.0 kN). Average values of *Fy* and *dy* in the comparison of RF-M and RF-MF specimens are very alike, which exposes the fact that the activation of Type B units as a fuse was not achieved. Consequently, the desired separation of infill and frame was not realized. The average ultimate drift of RF-M and RF-M is 2.5%.

Specimen label	Infill type	S_0 (kN/m)	F_y (kN)	F_u (kN)	d_{max} (mm)
RF	-	3.1	69.4	81.5	69.0
RF-M	RBA-EP Type A	14.4	64.9	128.0	48.7
RF-MF	RBA-EP Types A and B	14.3	68.3	132.3	59.9
PF-M	RBA-EP Type A	7.6	21.1	52.8	46.8

Table 4: Experimental results of the specimen with newly developed units

Figure 5 presents an even more detailed behavior of all specimens with RBA-EP units [14]. All tested specimens provide a much higher initial stiffness than the bare frame. Despite the higher initial stiffness of the pinned steel frame, the ultimate lateral load is much lower than for RF. From the PF-M envelope curve, it can be observed (especially on the positive side of the envelope) that there are frequent changes in behavior, which can illustrate the consequent re-distribution of the loads in the masonry infill. Furthermore, it is obvious that the contribution of the infill in the pinned frame cannot be simply added to the bare frame to achieve the structural behavior of the infilled frames. As for rigid frame specimens (RF-M and RF-MF), the envelope is smoother and there is symmetry in the negative and positive sides of envelopes. It can be also observed that RF-M and RF-MF specimens have high ductility (maximum drift ratio 2.1%-3.7%).

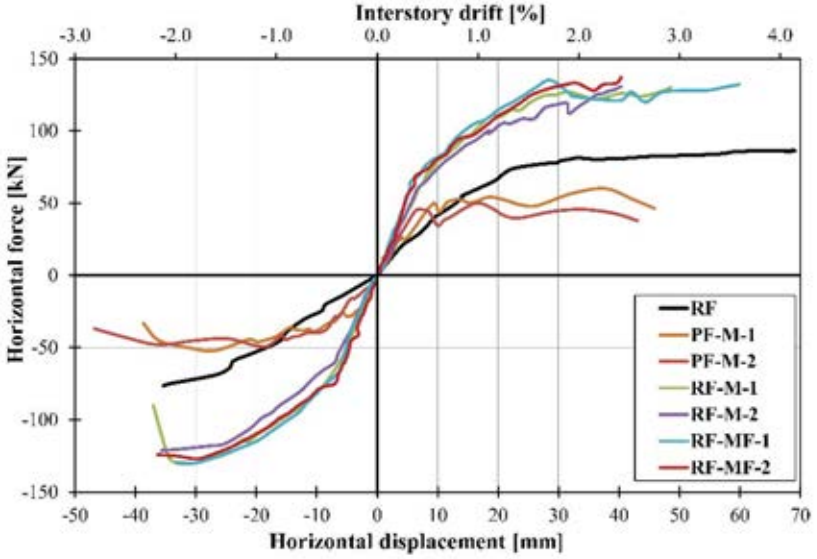

Figure 5: Hysteresis envelope curves of specimens

Regarding the fracture mechanism, RF-M and RF-MF again showed similarities. Dominated fracture mechanism on the change of initial stiffness is the diagonal formation of concentrated strain, and it is in line with mortar head and bed joints. Moreover, the configuration of RF-M and RF-MF ensures the composite system behavior in the quasi-elastic area, but without significant damage to the frame [14]. The highest concentration of strain in PF-M is also observed at the diagonals, but it is also spread over the whole panel. In terms of out-of-plane stability during in-plane loading, it is noticed that perforated units are more prone to out-of-plane stability issues (e.g., hollow clay brick). Despite that, the RBA-EP unit did not present that issue. This can be associated with their low elastic modulus and thick sidewalls [25].

6 COMPARISON OF RESULTS

The experimentally obtained average values of initial stiffness, load at the start of yielding, ultimate load, and maximum drift ratio are summarized in Table 5. It can be noticed that the average values of RF-C specimens, RF-C, provides the highest initial stiffness among all tested specimens, which was expected based on the highest compression strength of the masonry units and the modulus of elasticity of the masonry wallet. The lowest initial stiffness was achieved in the specimen with RBA-EP units, as was planned, but the ultimate load does not deviate from other specimens. Consequently, the authors successfully manipulated the properties of RBA-EP in which ultimate lateral bearing capacity is not significantly reduced. This similar behavior

is presented in the values of RF-A which had the highest ultimate load. Through the ultimate drift ratio, as a measure of ductility, it can be observed that specimens with RBA-EP units are more ductile than the rest of the specimens. The average value of the ultimate drift ratio for RF-M and RF-MF is 2.5%, while for RF-A and RF-C is 1.7% and 1.39% respectively. The lowest drift ratio is observed in RF-C_{av} specimens which had the highest initials stiffness. At the cost of ductility, higher initial stiffness is not a favorable property of infill. RF-M and RF-MF specimens additionally show similarity to the RF-A values in terms of compactness of the infill panel (e.g., no falling out of blocks, redistribution of stress through the infill). Besides numerous similarities, the difference is observed in the onset cracking. in the value of RF-A indicates that it happens earlier, while in RF-M and RF-MF the value of F_y is similar to the bare frame, but with different values of displacement. This confirms that the configuration of the specimens with RBA-EP preserved the steel frame from higher detrimental effects.

Specimen label	S_0 (kN/m)	F_y (kN	F_u (kN)	$D_{r,max}$ (%)
BF	3.1	69.4	81.5	3.25
RF-C_{av}	31.3	60.0	135	1.39
RF-A_{av}	19.83	51.3	146	1.74
RF-M	14.4	64.9	128.0	2.50
RF-MF	14.3	68.3	132.3	2.65
PF-M	7.6	21.1	52.8	2.70

Table 5: Comparison of initial stiffness and ultimate load

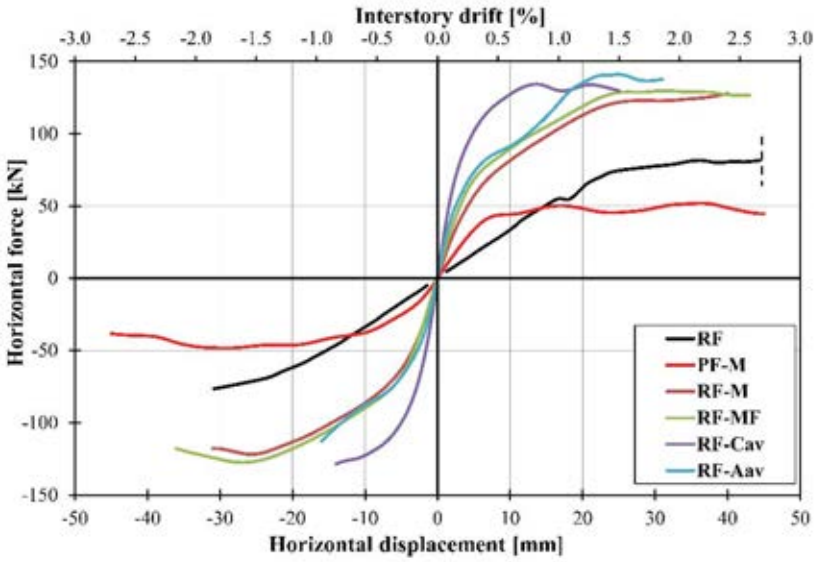

Figure 6: Hysteresis envelope curves of all tested specimens

Figure 6 [14] presents the hysteresis envelope curves of all tested specimens with different type of infills. It confirms a higher ultimate load in the presence of infill but with very different drifts. It can be noticed that RF-C value quickly attains the ultimate load which leads to an earlier onset of the failure mechanism. The hysteresis curve offers one more similarity between RF-M, RF-MF, and RF-A – trilinear behavior which ensures gradual redistribution of stress.

Through the experiments, it is once again confirmed that an infill panel plays an important role in the behavior of an infilled frame concerning the seismic design and that there is no adequate codified design method.

7 CONCLUSIONS OF CONDUCTED EXPERIMENTAL TESTS

A comparison of experimental programmes from previous studies is shown in this paper – rigid steel infilled frames with various types of infill, pinned steel frame, and a bare steel frame. The infill was made of hollow clay blocks, AAC blocks, and newly developed RBA-EP blocks. The experimental results show that simple construction provisions can lead to better behavior. Results can be summarized into the following conclusions:

- Infill provides a higher stiffness to the frame. Among all tested specimens, the highest initial stiffness was obtained in the RF-C configuration, which was expected because of the significantly higher compressive strength of hollow clay blocks. Despite higher initial stiffness, the ductility of these frames was lower. Lower initial stiffness did not negatively influence the ultimate strength of RF-A, RF-M, and RF-MF specimens. Consequently, the behavior of RF-A, RF-M, and RF-MF specimens is favorable.
- In terms of ductility, frames with RBA-EP units achieve higher ductility than RF-A specimens, which is manifested through ultimate drift. The average ultimate drift of RF-M and RF-MF specimens is 2.5%, which is 30% higher than RF-A.
- RBA-EP units are heavier in comparison to the AAC and hollow clay blocks, but they are environmentally favorable because they use waste products (recycled crush brick and polystyrene) in their production.
- Regarding the PF-M configuration, the results deviate in comparison to the rigid configurations, especially in terms of the ultimate load and the change of initial stiffness. Beyond that, the observed concentration of strain is spread over the whole panel and the stress state does not coincide with the infill in a rigid frame. Through this configuration, it is concluded that the bearing capacity of an infilled frame also depends on the rotation capacity of joints.
- Regarding the numerical models, it can be concluded that SSM and MSM can give good predictions in the case of C units, with a lack of accuracy for AAC units. Despite that, they still represent an acceptable method based on simplicity regarding the rest of the methods (fast calculation, the capability of producing hysteresis behavior). AMM and SPM models predict behavior much better with the included various types of failure mechanisms. Although the obtained results are better, the required time and complexity are important setbacks.

In future work, experimental tests of specimens with RBA-EP should be accompanied by numerical models to compare with C and AAC units. Furthermore, probabilistic methods should be conducted to evaluate the reliability of this type of structural concept.

REFERENCES

[1] D. Markulak, I. Radić, V. Sigmund, Cyclic testing of single bay steel frames with various types of masonry infill, *Engineering Structures,* **51**, 267–277 (2013).

[2] S. Pul, M.E. Arslan, Cyclic behaviors of different type of hollow brick infill walls: A hinged rigid frame approach, *Construction and Building. Materials,* **211**, 899–908 (2019).

[3] S.V.S. Jebadurai, D. Tensing, P.M. Pradhan, G. Hemalatha, Enhancing performance of infill masonry with latex modified mortar subjected to cyclic load, *Structures,* **23**, 551–557 (2020).

[4] B. Binici, *et al.* Seismic behavior and improvement of autoclaved aerated concrete infill walls, *Engineering Structures,*. **193**, 68–81 (2019).

[5] R.S. Ju, H.J Lee, C.C. Chen, C.C. Tao, Experimental study on separating reinforced concrete infill walls from steel moment frames, *Journal of Construction Steel Research,* **71**, 119–128 (2012).

[6] A.V. Tsantilis, T.C. Triantafillou, Innovative Seismic Isolation of Masonry Infills in Steel Frames using Cellular Materials at the Frame-Infill Interface, *Journal of Earthquake Engineering,* **24**, 1729–1746 (2020).

[7] M. Mohammadi, V. Akrami, R. Mohammadi-Ghazi, Methods to Improve Infilled Frame Ductility, *Journal of Structural Engineering,* **137**, 646–653 (2011).

[8] M. Preti, V. Bolis, A. Stavridis, Design of masonry infill walls with sliding joints for earthquake structural damage control, *Brick and Block Masononry: Trends, Innovations and Challenges - Proceedings of the 16th International Brick Block Masononry Conference, IBMAC 2016* 1317–1324 (2016).

[9] P. Morandi, R.R. Milanesi, C.F. Manzini, G. Magenes, Experimental tests of an engineered seismic solution of masonry infills with sliding joints, *16th World Conference on Eearthquake,* **4442**, (2017).

[10] M. Marinković, C. Butenweg, Innovative decoupling system for the seismic protection of masonry infill walls in reinforced concrete frames, *Engineering. Structures,* **197**, 109435 (2019).

[11] L. Silva, G. Vasconcelos, P. Lourenço, F. Akhoundi, Experimental evaluation of a constructive system for earthquake resisting masonry enclosure walls, *Brick and Block Masononry: Trends, Innovations and Challenges - Proceedings of the 16th International Brick Block Masononry Conference. IBMAC 2016* **2003**, 1333–1340 (2016).

[12] M. Aliaari, A.M. Memari, Analysis of masonry infilled steel frames with seismic isolator subframes, *Engineering. Structures,* **27**, 487–500 (2005).

[13] I.S. Misir, Potential Use of Locked Brick Infill Walls to Decrease Soft-Story Formation in Frame Buildings, *Journal of Performance of Constructed Facilitie,*. **29**, 04014133 (2015).

[14] D. Markulak, T. Dokšanović, I. Radić, J. Zovkić, Behaviour of steel frames infilled with environmentally and structurally favourable masonry units, *Engineering. Structures,* **204**, (2020).

[15] I. Radić, Ponašanje čeličnih okvirnih građevina sa zidanim ispunom pri djelovanju potresa. *PhD Thesis*. Osijek: Josip Juraj Strossmayer University of Osijek; 2012 [in Croatian].

[16] I. Radić, D. Markulak, V. Sigmund, Analitičko modeliranje čeličnih okvira sa zidanom ispunom, *Tehnički. Vjesnik,* **23**, 115–127 (2016).

[17] M.Y. Kaltakci, A. Koken, H.H. Korkomaz, An experimental study on the behaviour of infilled steel frames under reversed-cycling loading, *Iranin Journal of Sciece & Technology,* **32,** 157-160 (2008)

[18] H. A. Moghaddam, Lateral load behavior of Masonry infilled steel frames with repair and retrofit, *Journal of Structural Engineering,* **130**, 56-63 (2004)

[19] A.A. Tasnimi, A. Mohebkhah, Investigation on the behavior of brick-infilled steel frames with openings , experimental and analytical approaches, *Engineering Structures,* **33**, 968–980 (2011).

[20] R.D. Flanagan, R.M. Bennett, In-plane behavior of structural clay tile infilled frames, *Journal of Structural Engineering,* **125**, 590-599 (1999)

[21] M. Mohammadi, S.M.M Emami, Multi-bay and pinned connection steel infilled frames; an experimental and numerical study, *Engineering structures,* **188**, 43-59 (2019)

[22] Y. Liu, G. Li, Behavior of steel frames with and without AAC infilled walls subjected to static and cyclic horizontal loads, *13th World Conference on Eartquake Engineering,* **1112**, (2004)

[23] C. Zhenggang, P. Du, F. Feng, F. Ming, Cyclic testing and parametric analyses of the fabricated steel frames infilles with autoclaved aerated concrete panels, *Advance in Structural Engineering*, **20**, 473-490 (2016)

[24] S. Ravichandran, Design provisions for autoclaved aerated concrete (AAC) infilled steel moment frams, *Ph.D Dissertation.* Austin, Texas: The University of Texas at Austin

[25] D. Markulak, T. Dokšanović, I. Radić, I. Miličević, Structurally and environmentally favorable masonry units for infilled frames, *Engineering Structures,* **175**, 753–764 (2018).